International Journal of Pharmaceutics 395 (2010) 53–61

Contents lists available at ScienceDirect

International Journal of Pharmaceutics

journal homepage: www.elsevier.com/locate/ijpharm

Solid dispersion of acetaminophen and poly(ethylene oxide) prepared by hot-melt mixing

Min Yang[a], Peng Wang[a], Chien-Yueh Huang[c,1], M. Sherry Ku[c,1], Huiju Liu[a], Costas Gogos[a,b,*]

[a] The Otto H. York Department of Chemical, Biological and Pharmaceutical Engineering, New Jersey Institute of Technology, University Heights, Newark, NJ 07102, USA
[b] Polymer Processing Institute, Newark, NJ 07102, USA
[c] Pharmaceutical Development, Wyeth Research, Pearl River, NY 10965, USA

ARTICLE INFO

Article history:
Received 18 February 2010
Received in revised form 16 April 2010
Accepted 23 April 2010
Available online 7 May 2010

Keywords:
Hot-melt Mixing
Solid Dispersion
Recrystallization
Clay
Acetaminophen/paracetamol
PEO

ABSTRACT

In this study, a model drug, acetaminophen (APAP), was melt mixed with poly(ethylene oxide) (PEO) using a Brabender mixer. APAP was found to recrystallize upon cooling to room temperature for all the drug loadings investigated. Higher drug loading leads to faster recrystallization rate. However, the morphology of the recrystallized drug crystals is identical in samples with different drug loadings and does not change with the storage time. To adjust the drug's dissolution rate, nanoclay Cloisite® 15A and 30B were added into the binary mixture. The presence of either of the nanoclay dramatically accelerates the drug's recrystallization rate and slows down the drug's releasing rate. The drop of the releasing rate is mainly due to the decrease of wettability, as supported by the contact angle data. Data analysis of the dissolution results suggests that the addition of nanoclays changes the drug's release mechanism from erosion dominant to diffusion dominant. This study suggests that nanoclays may be utilized to tailor the drug's releasing rate and to improve the dosage form's stability by dramatically shortening the lengthy recrystallization process.

1. Introduction

Hot-melt extrusion (HME) has received a great deal of interest recently from the pharmaceutical industry for the preparation of solid drug dosage form (Andrews et al., 2008; Hülsmann et al., 2000; Li et al., 2006; Liu et al., 2010; Schilling et al., 2010). The process involves mixing active pharmaceutical ingredients (APIs) with molten polymeric excipients in processing machines with one or more rotating screws. HME possesses several unique advantages over traditional manufacturing processes. It is a continuous process and it eliminates or minimizes the solvent usage. Solid solutions or dispersions can be prepared to improve the bioavailability of APIs with poor water solubility. Since a large number of newly developed chemical entities are poorly soluble in water, it is understandable that much research effort has been devoted to utilizing the HME process to prepare drugs with enhanced bioavailability. On the other hand, it should be pointed out that HME potentially can be applied to manufacture solid dosage forms with a wide range of release profiles, considering the richness of the polymer chemistry and the powerful mixing and shaping capability of the extrusion process. For example, HME can be readily applied to prepare drugs with sustained release profiles, as demonstrated by previous studies (De Brabander et al., 2003; Özgüney et al., 2009; Yang et al., 2008; Verhoeven et al., 2009). Generally speaking, drug tablets prepared via HME can be less porous and have better mechanical properties, which are desirable for sustained release.

Many previous studies have demonstrated the feasibility and advantages of the HME process. Still, some challenges need to be addressed in order to have broader applications of HME in the industry. One challenge lies in the API's tendency to recrystallize after the temperature drops from the elevated processing temperature to room temperature. Depending on the specific application, different strategies can be employed to address the recrystallization issue. For example, if improving the drug's dissolution rate or solubility is not a concern, then the recrystallization may not bring any undesirable effects as long as the drug can quickly reach a physical stable state after the HME process. On the other hand, if the goal is to improve the drug's bioavailability via increasing the API's dissolution rate, then choosing appropriate excipients and/or optimizing the HME process is needed to improve the drug–polymer miscibility or dramatically slow down the recrystallization rate. For both cases, a better understanding of API's recrystallization process is prerequisite in order to prepare a drug with a desired releasing profile.

* Corresponding author at: The Otto H. York Department of Chemical, Biological and Pharmaceutical Engineering, New Jersey Institute of Technology, University Heights, Newark, NJ 07102, USA. Tel.: +1 973 642 7365.
E-mail address: gogos@polymers-ppi.org (C. Gogos).
[1] Current address: Pharmaceutical Development, Pfizer, Pearl River, NY 10965, USA.

0378-5173/$ – see front matter © 2010 Elsevier B.V. All rights reserved.
doi:10.1016/j.ijpharm.2010.04.033

In this study, poly(ethylene oxide) (PEO) and acetaminophen (APAP) were chosen as the model polymeric excipient and drug, respectively. The recrystallization phenomenon and the effects of nanoclay on the recrystallization were investigated. PEO, a semicrystalline polymer, is often chosen as the excipient for HME because of its broad processing window (Coppens et al., 2006). PEO has been used in applications such as sustained-release matrix systems, transdermal drug delivery systems, and mucosal bioadhesives (Prodduturi et al., 2005; Repka et al., 2003; Zhang and Mcginity, 1999). The model drug APAP, a pain reliever and fever reducer, has a solubility of 14.90 mg/g in water at 25 °C (Granberg and Rasmuson, 1999). PEO and APAP should be partially miscible based on the criteria suggested by Greenhalgh et al. (1999) and two materials' difference in solubility parameter, 7.46 $MPa^{1/2}$ to be exactly (Mididoddi and Repka, 2007; Breitkreutz, 1998).

In practice, it is often difficult to find one polymeric excipient that meets all the requirements in terms of processability, miscibility with the drug, and dissolution characteristics. Hence, a third component, such as a surfactant or layered silicate nanoplatelet, can be added for the purposes such as adjusting the release profile (Campbell et al., 2008; Ghebremeskel et al., 2006, 2007). In this study, two commercially available nanaclays, Cloisite® 15A and 30B were used. A Cloisite® particle of 8 microns contains over 1,000,000 platelets stacked together. Extremely large interfacial area between the clay and the polymer can be obtained if the platelets can be separated, also called exfoliated, from each other after the clay is processed together with a polymer. Because of this unique property, nanoclays are used in the polymer industry to slow down the diffusion of gaseous molecules inside various polymers. Cloisite® 15A is a natural montmorillonite modified with dimethyl, dehydrogenated tallow and quaternary ammonium cations, while Cloisite® 30B is a montmorillonite modified with bis-(2-hydroxyethyl) methyl tallowalkyl ammonium cations. Cloisite® 15A was found to intercalate in PEO and affect the PEO's crystallization (Homminga et al., 2005). The silicate layers acted as nucleating agents for the crystallization of PEO in low concentrations, and retarded the crystal growth at sufficiently high clay amounts (4 wt%). Melt-mixed PEO-Cloisite® 30B, on the other hand, formed exfoliated nanocomposites with no clear SAXS (small angle X-ray scattering) peaks of PEO and lower PEO crystallinity (Loyens et al., 2005). In summary, nanoclays present another route to tailor the drug's releasing rate without bringing any significantly undesirable impact on the HME process. Thus it is worthwhile to undertake a fundamental investigation of the effects of nanoclays on the polymer-drug system.

2. Experimental

2.1. Materials

The crystalline APAP powders with a melting temperature ~170 °C were purchased from Spectrum Chemicals (Gardena, CA). PEO N10 ($M_w = 1 \times 10^5$ g/mol), a semicrystalline polymer with $T_g \sim -54$ °C and $T_m \sim 60$ °C, was donated by the Dow Chemical Co. (Midland, MI). Nanoclays Cloisite® 15A (referred as 15A) and Cloisite® 30B (referred as 30B) were donated as samples from Southern Clay Products (Gonzals, TX).

2.2. Preparation of hot-melt mixed samples

In this study, a Brabender FE-2000 batch mixer (Messrs. C.W. Brabender Instruments Inc., South Hackensack, NJ) was used to mix the different materials. The batch mixer has two counter-rotating screws, impacting mixing similar to that generated in twin-screw extruders. That is why the batch mixer is commonly used in the plastics industry for small scale testing before scaling up to a continuous extruder. The mixer is heated electrically and cooled by air. The equipped temperature sensor measures the actual melting material's temperature; the torque meter records the resistance to the screw's rotation caused by the presence of the materials. One big advantage of using the batch mixer instead of a continuous extruder is that the residence time can be controlled separately from other processing parameters such as the screw speed, although the effect of the residence time is beyond the scope of this article. 50 g of materials, be it PEO, APAP–PEO, or APAP–nanoclay–PEO powder (about 70% of total free volume of the chamber), was processed in each batch. The composition and the acronym names of the sample are given in Table 1. The processing temperature was kept at 100 °C and the rotor speed of screws was controlled at 50 rpm by a computer program. After 6 min of mixing, the samples were taken out of the batch mixer and pressed immediately into ~2 mm thick discs, which were then cooled down to room temperature in the open air.

Table 1
Samples prepared by hot-melt mixing.

Sample name	Composition	Weight ratio	Cooling medium
100PEO	PEO	–	Open air
10APAP	APAP:PEO	1:9	
10APAP10CL15A	APAP:Cloisite 15A:PEO	1:1:8	
10APAP10CL30B	APAP:Cloisite 30B:PEO	1:1:8	
20APAP	APAP:PEO	2:8	
20APAP10CL15A	APAP:Cloisite 15A:PEO	2:1:7	
20APAP10CL30B	APAP:Cloisite 30B:PEO	2:1:7	
30APAP	APAP:PEO	3:7	
30APAP10CL15A	APAP:Cloisite 15A:PEO	3:1:6	
30APAP10CL30B	APAP:Cloisite 30B:PEO	3:1:6	
20APAP-LN	APAP:PEO	2:8	Liquid N_2
20APAP-air	APAP:PEO	2:8	Open air

To understand the effect of cooling rate, some fresh-made samples were dropped into liquid nitrogen and kept for 3 min. The frozen sheets were then warmed to room temperature in the open air. All samples were stored at room temperature in a vacuum dessicator with silica gel.

2.3. Characterization

2.3.1. Thermal gravimetric analysis (TGA)

TA Instruments Q50 thermogravimetric analyzer (TGA) (New Castle, DE) was utilized to study the chemical stability of PEO and APAP at elevated temperatures. In ramp heating tests, 2–10 mg of powders were placed in an aluminum pan and heated from room temperature to 250 °C at a heating rate of 10 °C/min. In isothermal heating tests, powders were quickly heated to 100 °C at a rate of 50 °C/min and held isothermally for 10 min. The chamber was flushed with air at a flow rate of 40 ml/min during the testing.

2.3.2. Polarized optical microscopy (POM) and hot-stage microscopy (HSM)

Morphology of samples was investigated using a polarized optical microscope (Carl Zeiss SMT Inc., Peabody, MA) equipped with a Zeiss AxioCam MRc5 (5 MB-pixel resolution) digital camera. Dissolution of crystalline APAP in molten PEO was observed by using the hot-stage microscope (Mettler-Toledo Inc., Columbus, OH). The mixture samples were placed between two glasses and heated from room temperature to 100 °C at 10 °C/min. Images were taken during the heating process.

2.3.3. Scanning electron microscopy (SEM)

Morphologies of samples were examined using a LEO 1530 Field Emission Scanning Electron Microscope (Carl Zeiss SMT Inc.,

Peabody, MA) at 2 keV. Both the surface and cryo-fracture of the samples were characterized. The cryo-fractures were prepared by snapping a sample disc that had been soaked in liquid nitrogen for 5 min. All samples were sputtered with a thin layer of carbon to improve the electrical conductivity prior to imaging.

2.3.4. X-ray diffraction (XRD)

Philips PW3040 X-ray diffractometer (PANalytical Inc., Westborough, MA) was controlled by X'Pert software with Cu Kα radiation (λ = 1.54 Å) generated from a copper source operating at a power level of 40 KV and 40 mA. The sample discs were held directly for XRD analysis and scanned over the 2θ range of 5–30° at the step size of 0.03°/step and the scan rate of 1 second/step. The slit configuration was 1.0°, 1.0° and 0.1 mm for divergence, anti-scatter and receiving slit, respectively.

2.3.5. Differential scanning calorimetry (DSC)

DSC measurements were carried out using a TA Instruments Q100 (New Castle, DE) equipped with a refrigerated cooling system. The chamber was flushed with N_2 at a flow rate of 40 ml/minute during the testing. About 4 mg sample was weighed and placed in an aluminum pan with lid and crimp sealed. Samples were heated from 0 to 200 °C at the rate of 10 °C/min and all the tests were carried out in triplicate.

2.3.6. Dissolution testing

Dissolution tests were performed under the sink condition using a Distek 2100A USP standard dissolution apparatus with a basket stirrer. The dissolution medium (900 ml of aqueous buffer solution with pH 7) was maintained at 37 ± 0.5 °C and stirred at 50 rpm. At predetermined intervals, 5 ml of solution was withdrawn and the volume change was corrected in the calculation. The liquid was filtered with a Millipore 0.45 μm PVDF filter and analyzed using 10 mm quartz cells and an Agilent 8453 UV Spectrophotometer (Foster City, CA) at 243 nm. The tests were performed three times to check repeatability.

2.3.7. Contact angle measurement

Water contact angle measurements were carried out at room temperature with a model 100-00 contact angle goniometer (Rame-Hart, Inc., Netcong, NJ). The contact angles were recorded immediately after dispensing ~10 μL water droplets with a pipet onto the surface. The reported values were average values of measurements for more than three different samples at more than three different locations for each composition.

3. Results and discussion

3.1. Hot-melt mixing

Table 1 summarizes the samples prepared using the batch mixer in this study. The materials' thermal stability was investigated via the TGA test. The onset temperatures of weight loss in the TGA ramp heating tests are above 150 °C for 30 wt%APAP–PEO powder mixture, APAP and PEO (Fig. 1a). In addition, isothermal tests show no weight loss at 100 °C for 10 min in the air environment (Fig. 1b). In this study, all samples were processed for 6 min at 100 °C, which is way below the materials' degradation temperature.

The evolution of the torque during mixing of 30APAP is given as an example in Fig. 2. The increase of the torque at the beginning represents the feeding surge. After that, the torque value decreases until it reaches a plateau. It takes about 5 min for the torque to reach a constant value. The drop of the torque is due to the viscosity decrease of the mixture, which is caused not only by the melting of PEO, but also by the dissolution of the APAP molecules into the highly viscous polymer melt. Detailed rheological results will be a part of another paper currently under preparation. Simply put, the dissolved APAP acts as a plasticizer, thus lowering down the viscosity of the mixture. Finally, a constant torque value indicates the completion of the drug's dissolution process. In all the experiments, materials were mixed for 6 min.

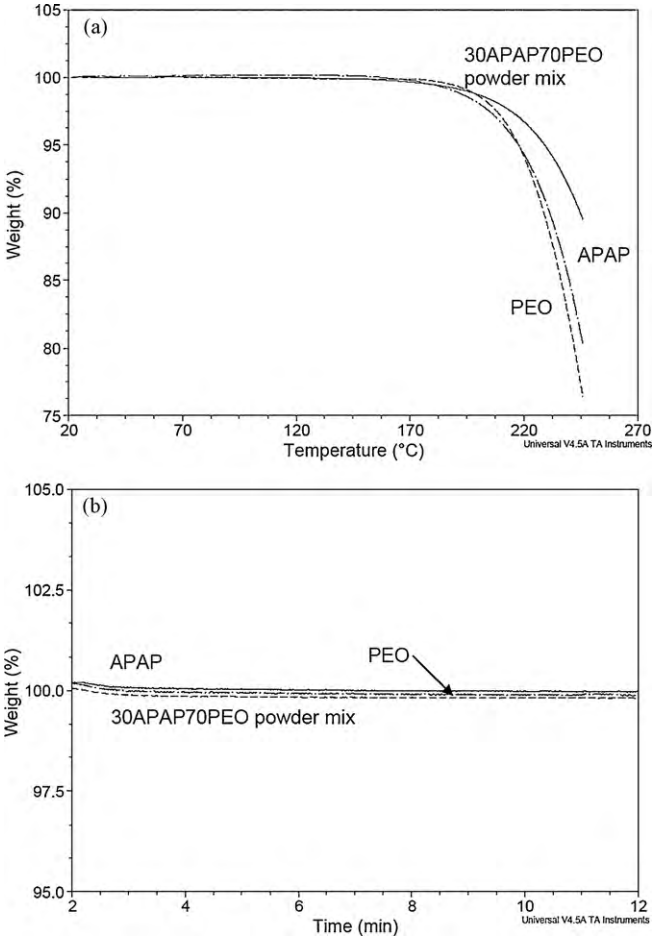

Fig. 1. TGA thermograms of APAP, PEO and 30 wt% APAP–PEO powder mix in air (a) ramp heating at 10 °C/min; (b) isothermal heating at 100 °C for 10 min.

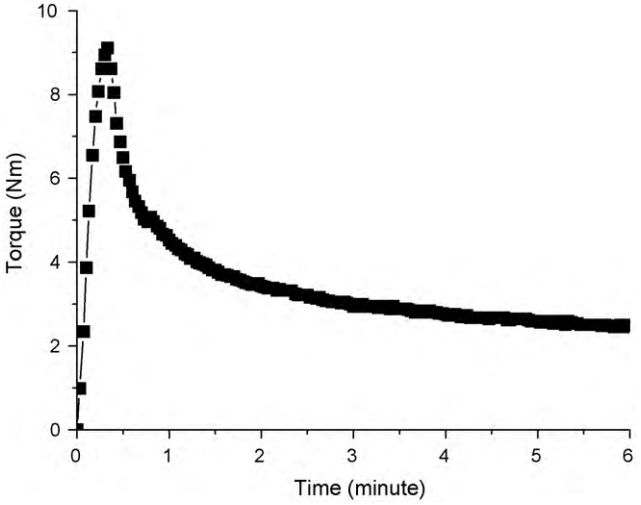

Fig. 2. The evolution of torque during melt mixing (30APAP).

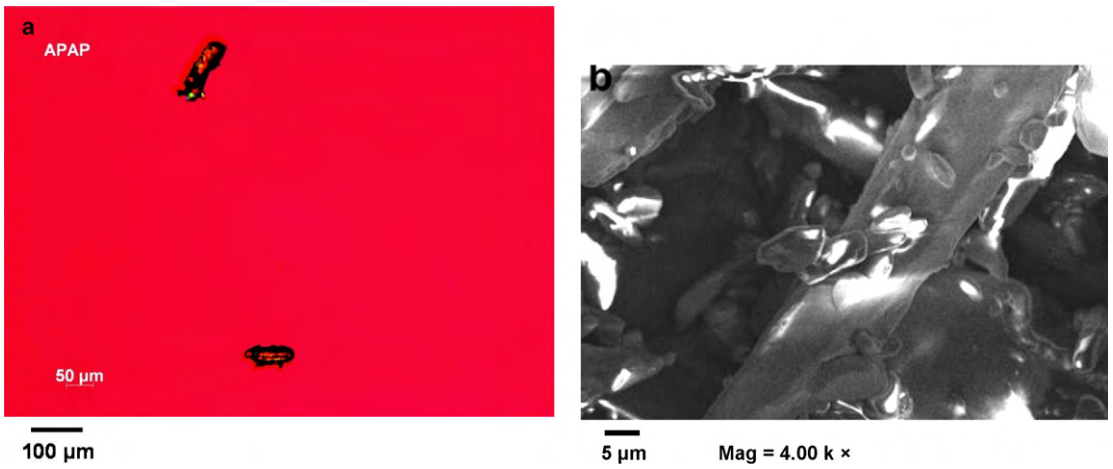

Fig. 3. (a) POM and (b) SEM image of acetaminophen powders.

3.2. POM and SEM

The original APAP powders are needle-shape crystals, with the length *ca*. 50–100 μm (Fig. 3a). Since the particles are quite brittle, the drug powders also include a significant amount of fine powders, ~2 μm in size (Fig. 3b).

All freshly made sample discs have a light yellow color, the same as pure PEO sample processed under the same conditions. However, unlike the pure PEO, the color of mixture will gradually change to milky white at room temperature, suggesting the occurrence of APAP's recrystallization after processing. The rate of the color change is dependent on the APAP concentration: the appearance of 20APAP and 30APAP samples changes appreciably within several hours, whereas it takes days for 10APAP samples to have appreciable visual changes. SEM photos reveal what happens at the micro scale. Fresh-made 10APAP has a relatively smooth and particle-free surface (Fig. 4a). On the contrary, drug particles, about 1–3 μm in size, are found on the surfaces of 20APAP (Fig. 4b-c) and 30APAP after the same storage time. SEM images of cryo-fracture samples suggest that APAP also recrystallizes at the interior of all samples (pictures not shown). It should be mentioned that after 18 days of storage, drug particles also appear at the surface of 10APAP (Fig. 5). The size of drug particles in 20APAP and 30APAP does not change over time.

The recrystallization of APAP can be roughly divided into two stages according to the recrystallization rate. For 20APAP and

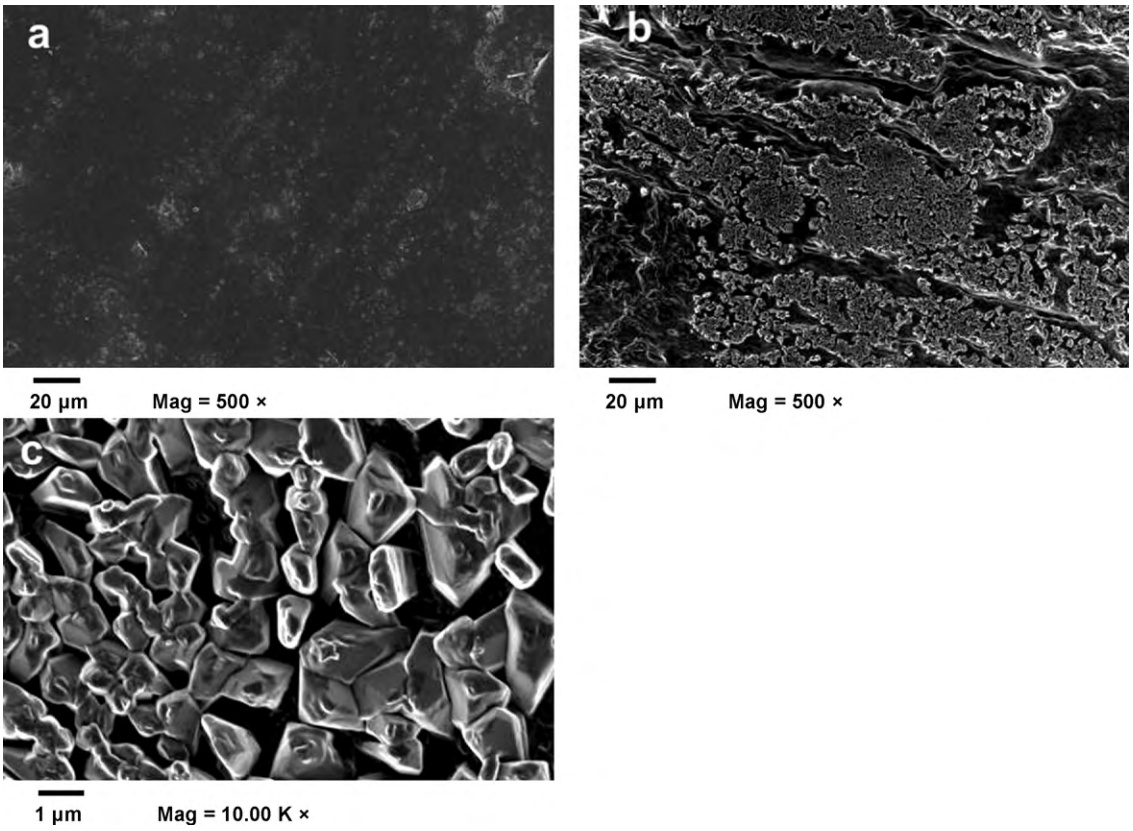

Fig. 4. SEM images of fresh-made sample (3 h after melt mixing) (a) 10APAP Mag = 500×; (b) 20APAP Mag = 500×; (c) 20APAP Mag = 10,000×.

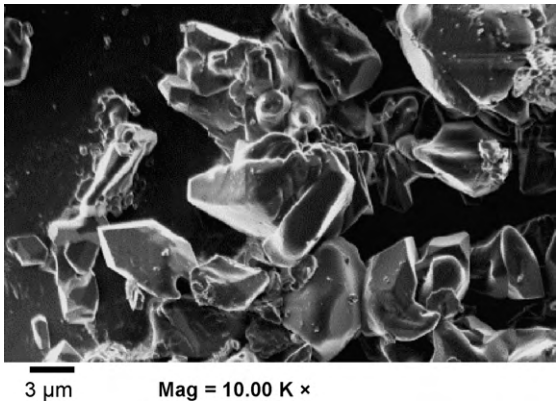

Fig. 5. SEM images of 10APAP after stored for 18 days.

30APAP samples, the first stage takes only several hours, whereas for 10APAP, the first stage takes weeks. After the first stage, the systems still have not reached thermodynamic equilibrium. However, the recrystallization rate drops significantly in the second stage.

The morphology of the recrystallized APAP particles is of great importance since it may affect the drug's dissolution rate in an aqueous medium. For the APAP–PEO system cooled at room temperature, APAP particles formed from recrystallization have identical morphologies among samples with different drug loadings. The APAP particles are about several micrometers in size and dispersed throughout the polymeric matrix. The drug loading does not affect the morphology of drug particles formed during recrystallization in this system. Cooling rate is another parameter that may affect the morphology of recrystallized drug particles. To investigate the effect of the cooling rate on recrystallization, 20APAP samples were cooled in two different cooling media: open air and liquid nitrogen. Fig. 6 suggests that different cooling rates lead to different morphologies of recrystallized drug particle. Dispersed drug particles, of around several microns in size, are generated in the slowly cooled samples. While for the quenched sample, drug molecules grow into interconnected snowflake-like structures. The results suggest that the cooling rate does affect the drug particle morphologies and needs to be carefully controlled in practice. In some drug–polymer systems, an extremely fast cooling rate may slow down the molecular mobility so much that the recrystallization becomes almost undetectably slow. Apparently it is not the case for PEO–APAP system, which may due to the extremely low glass transition temperature of PEO.

In summary, the experimental results suggest that APAP recrystallizes for all three concentrations tested. The size and the shape of the recrystallized APAP particles are independent of the drug loading. However, the cooling rate does affect the drug particles' morphology to some extent.

3.3. XRD

Samples with 20 and 30 wt% of APAP share the same XRD patterns. Fig. 7 shows the XRD spectra of the binary and ternary APAP–PEO mixtures with 30% drug loading. The solid state of APAP has been intensively investigated (De Wet et al., 1998; Lang et al., 2002). In this study, APAP are in monoclinic form in all samples. Consistent with the SEM observations, APAP quickly recrystallizes within the first day of storage, after which the recrystallization becomes extremely slow. APAP crystalline peaks in samples with 10 wt% APAP, on the other hand, are very weak and it is difficult to draw any conclusions regarding the recrystallization rate (spectra not shown).

Adding nanoclays into the APAP–PEO mixture dramatically accelerates the recrystallization process of APAP (Fig. 7b–c). As mentioned earlier, two nanoclays, Cloisite® 15A and Cloisite® 30B, were used in the study. Among all the modified Cloisite® series nanoclays, Cloisite® 15A is the most hydrophobic and Cloisite® 30B the most hydrophilic. However, the hydrophobicity difference does not appear to play a significant role in this case. Two nanoclays are essentially identical in terms of impact on the APAP's recrystallization. Nanoclay particles act as nucleation agents and allow the APAP recrystallization process to complete within a much shorter time. No further change in APAP's solid state is observed during the next sixty days, based on the results from XRD and SEM. The finding suggests that potentially nanoclays can be employed to prepare more stable tablets.

It should be mentioned that nanoclay can also affect the polymer's crystallization rate to various degrees, depending on the polymer–nanoclay system. For example, the addition of silicate layers can induce hetero-phase nucleation and promote the growth of polyamide crystallites (Liu and Wu, 2002). Another study has shown that the crystallization kinetics of polyamide nanocomposites increases only when clay concentrations are very low, while high clay loadings retard the crystallization by restricting lamellae coarsening in PEO (Fornes and Paul, 2003). The clay particles act as a nucleating agent for maleic anhydride grafted polypropylene, but do not influence the linear growth rate of spherulites or overall crystallization rate significantly (Maiti et al., 2002). The APAP–PEO-clay is a more complicated system comprising several phases, including layered silicate, amorphous APAP and PEO regions, crystalline PEO regions and crystalline APAP regions. The nanoclays significantly facilitate APAP crystallization; while slightly inhibit PEO's crystallization, as evident by the DSC results.

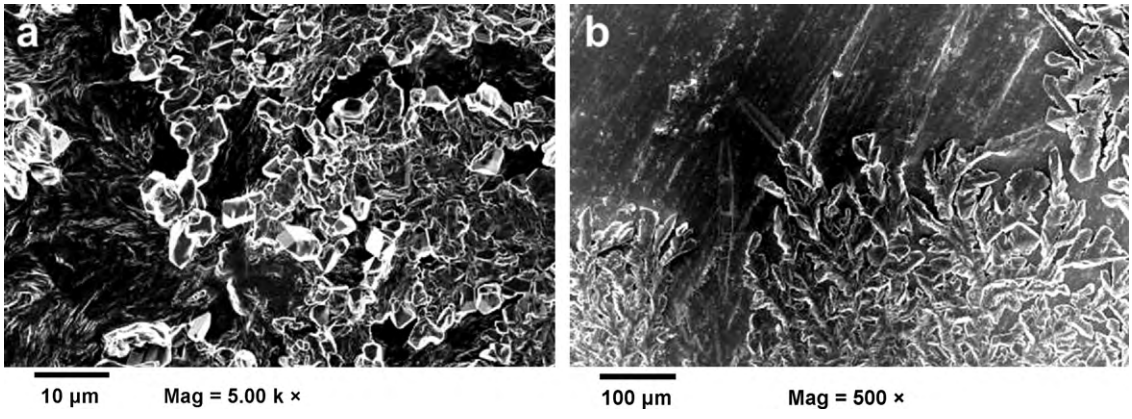

Fig. 6. SEM images of samples cooled in different media: (a) 20APAP-air and (b) 20APAP-LN.

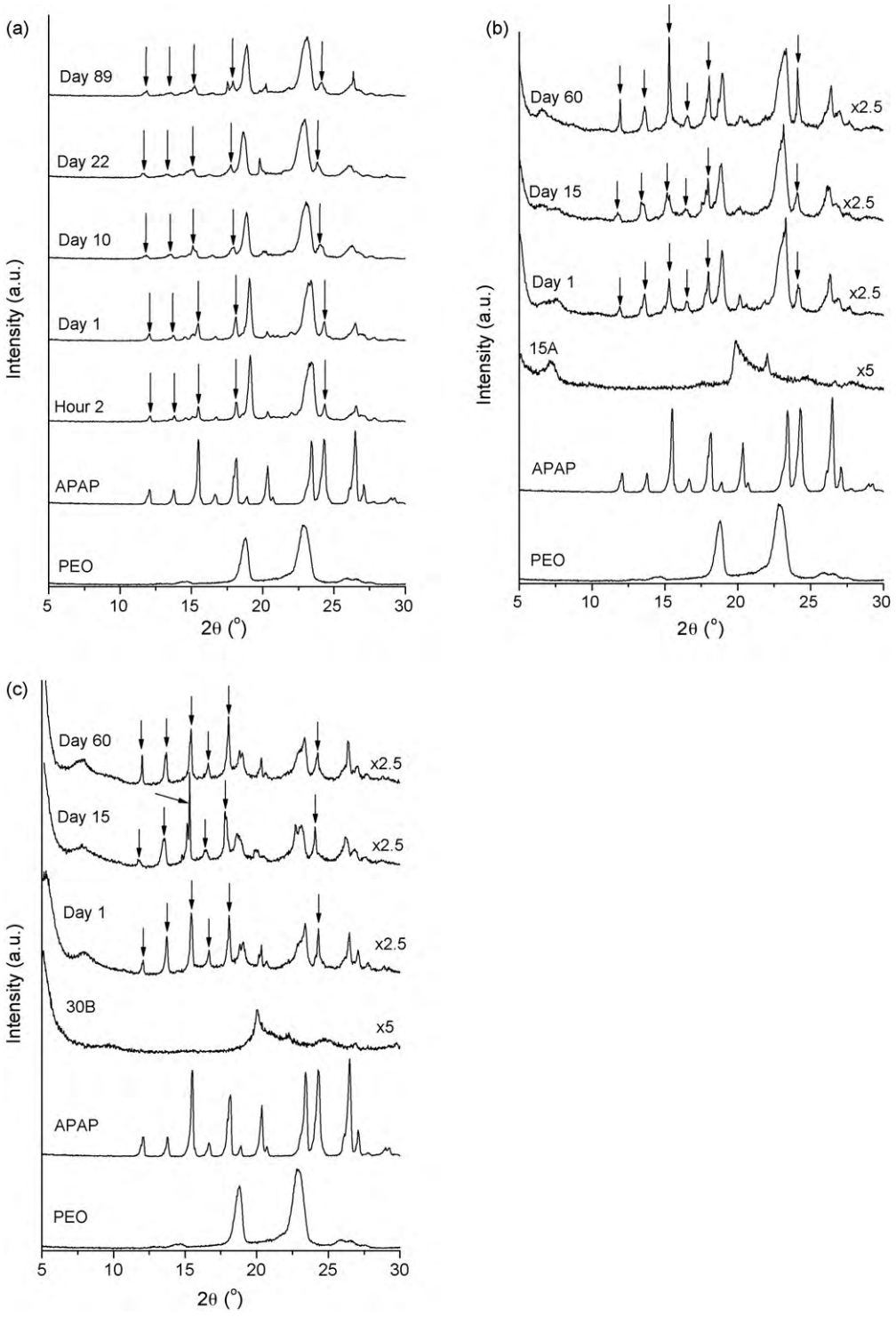

Fig. 7. XRD spectra of melt-mixed samples with 30 wt% APAP: (a) 30APAP; (b) 30APAP10CL15A; (c) 30APAP10CL30B.

3.4. DSC and HSM

All DSC thermograms of binary and ternary melt-mixed samples, regardless of APAP concentration, display only the melting peak of PEO. Fig. 8 depicts the DSC thermograms of 30APAP that has been stored for 2 and 74 days. The absence of endothermic peaks of APAP cannot be attributed to the drug being amorphous because both SEM and XRD results have proven the otherwise. A rational explanation is that crystalline APAP gradually dissolves into the molten PEO during the thermal scan. By the time the temperature reaches the melting point of APAP, there is no crystalline APAP left for detectable endotherms to appear on the thermoanalytical curves. This theory was confirmed by HSM observation, where recrystallized APAP was found to dissolve in molten PEO far below APAP's melting temperature: hot-stage microscopic pictures in Fig. 9 show the dissolution process of crystalline APAP from 80 to 100 °C. This finding is consistent with that described in an earlier publication (Lloyd et al., 1997), where APAP was observed to begin to dissolve into PEG 4000 as soon as the carrier was melted. As a result, DSC, a commonly used tool for determination of drug's crys-

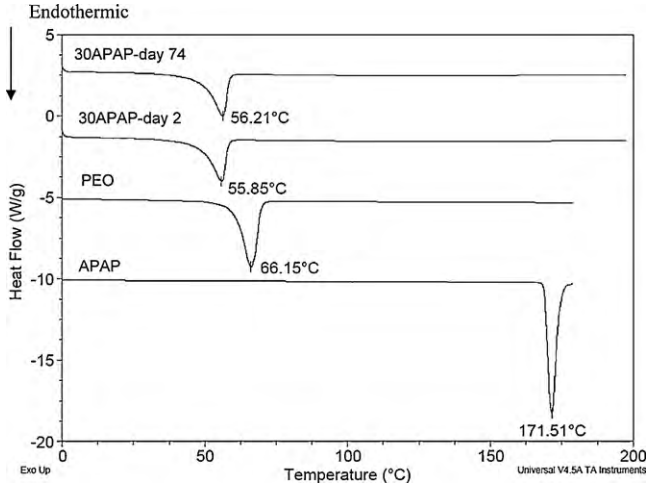

Fig. 8. DSC thermograms of pure APAP powder, melt-mixed 100PEO, 30APAP-day 2 and 30APAP-day 74 (from bottom to top).

talline state, cannot be applied for the APAP–PEO system. On the other hand, PEO peaks are clearly visible on the DSC thermograms. The melting enthalpy of the PEO suggests that adding nanoclay only slightly decreases the degree of crystallinity of PEO (results not shown).

3.5. Dissolution test

The dissolution rates of APAP–PEO and APAP–nanoclay–PEO are much slower than that of pure APAP powder in capsule, as shown in Figs. 10–12. It takes less than 30 min for powder-form APAP to be fully released into the buffer solution, while it takes melt-mixed APAP–PEO 90 min and APAP–nanoclay–PEO more than 6 h, an order of magnitude slower, to be fully dissolved.

Diffusion, swelling and erosion are the most important rate-controlling mechanisms of commercially available controlled-release products (Langer and Peppas, 1983). In order to understand the mode of drug release from PEO matrices, the data (M_t/M_∞) are fitted using the following power law (Siepmann and Peppas, 2001; Peppas and Korsmeyer, 1986; Ritger and Peppas, 1987; Crank, 1975):

$$\frac{M_t}{M_\infty} = kt^n \quad (1)$$

M_t, M_∞, k and n are respectively the amounts of drug released at time t, the absolute cumulative amount of drug released at infinite time, a constant incorporating the structural and geometric characteristics of the release device, and the exponent of the release kinetics. This semi-empirical equation was used to analyze the first 60% of a release curve ($M_t/M_\infty \leq 60\%$). The values of n were obtained by fitting drug release data to Eq. (1) using the ordinary least square regression (values ± 95% confidence limits) provided by software Polymath 5.1 (Polymath software, Willimantic, CT). For a disc, $n = 0.5$ suggests a diffusion-controlled-release mechanism and zero order drug release indicates an erosion-controlled-release mechanism. Anomalous transport leads to a value between 0.5 and 1.

The values of n for APAP release are listed in Table 2. It is interesting that the exponent n decreases from 1 for APAP–PEO system to about 0.7 for APAP–nanoclay–PEO mixtures, indicating the drug release shifts from erosion dominant to anomalous by addition of nanoclays.

Another equation developed by Peppas and Sahlin (Peppas and Sahlin, 1989; Hopfenberg and Hsu, 1978) (Eq. (2)) can be used to estimate the contributions of drug diffusion and polymer erosion to the anomalous release.

$$\frac{M_t}{M_\infty} = k_1 t^m + k_2 t^{2m} \quad (2)$$

The first term on the right hand side represents the contribution of drug diffusion and the second term the contribution of polymer erosion. The coefficient m is the diffusion exponent for a controlled-release device of any geometrical shape exhibiting pure drug diffusion. The value of m for the disc (or film) is 0.5 according to Peppas and Sahlin. Drug release data are fitted to Eq. (2) using the software Polymath 5.1. k_1 and k_2 are the diffusion and relaxation constant, respectively.

The results show that APAP diffusion has a much higher contribution than polymer erosion ($k_1 \gg k_2$) (Table 2) for the ternary mixture. The difference in drug release mode between the binary

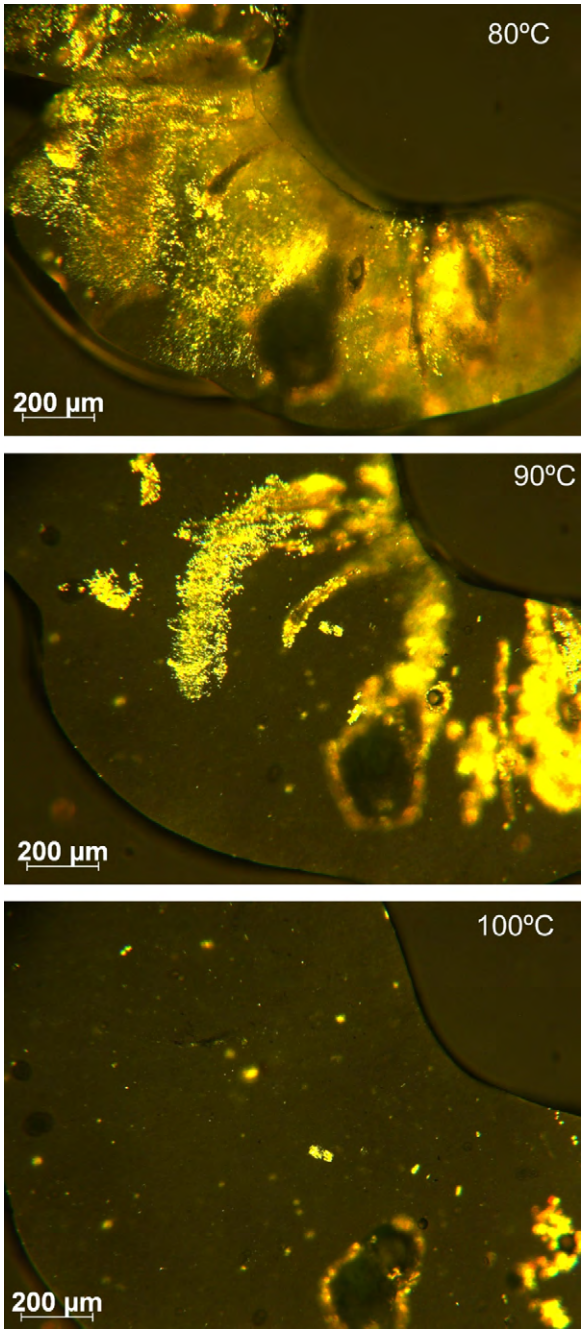

Fig. 9. Polarized microscopic images of 20APAP on the hot stage at 80, 90 and 100 °C.

Table 2
Fitting results for Eqs. (1) and (2). In all cases R^2 is greater than 0.99.

Sample	Power law $\frac{M_t}{M_\infty} = kt^n$	Peppas and Sahlin $\frac{M_t}{M_\infty} = k_1 t^{0.5} + k_2 t$	
	$n \pm 95\%$ CI	k_1 (% min$^{-0.5}$) $\pm$ 95% CI	k_2 (% min^{-1}) $\pm$ 95% CI
10APAP-day 1	1.02 ± 0.01	−0.16 ± 0.29	1.01 ± 0.05
20APAP-hour 1	0.89 ± 0.06	1.40 ± 1.11	1.25 ± 0.21
30APAP-hour 1	0.89 ± 0.03	1.57 ± 0.61	1.26 ± 0.12
10APAP10CL15A-hour 1	0.71 ± 0.02	2.13 ± 0.26	0.21 ± 0.03
10APAP10CL15A-day 251	0.56 ± 0.03	4.16 ± 0.29	0.07 ± 0.03
10APAP10CL30B-hour 1	0.70 ± 0.01	2.63 ± 0.37	0.21 ± 0.04
20APAP10CL15A-hour 1	0.67 ± 0.03	3.66 ± 0.61	0.21 ± 0.07
20APAP10CL15A-day 212	0.71 ± 0.01	2.44 ± 0.24	0.22 ± 0.02
20APAP10CL30B-hour 1	0.72 ± 0.02	2.63 ± 0.47	0.23 ± 0.05
30APAP10CL15A-hour 1	0.68 ± 0.01	3.02 ± 0.42	0.24 ± 0.05
30APAP10CL15A-day 213	0.71 ± 0.02	2.52 ± 0.42	0.25 ± 0.05
30APAP10CL30B-hour 1	0.69 ± 0.06	3.52 ± 1.07	0.33 ± 0.14

and ternary mixtures is postulated to be caused by the decrease of wettability with the presence of nanoclays. It should be noted that the nanoclays are modified by the suppliers to improve their compatibility with polymers. The modified clays are more hydrophobic than the original montmorillonite. Experimental results show that the contact angle of dissolution medium on the surface of 10APAP is 41°, ten degree smaller than that on the surface of 10APAP10CL15A or 10APAP10CL30B. The decrease in wettability dramatically slows down the dissolution rate of the matrix: for APAP–PEO system, the full release of APAP and the complete dissolution of matrix occur at the same time, roughly 1 h from when the sample was immerged in the solution. In comparison, the matrix of the ternary mixture remains even after 6 h, when all APAP has been released.

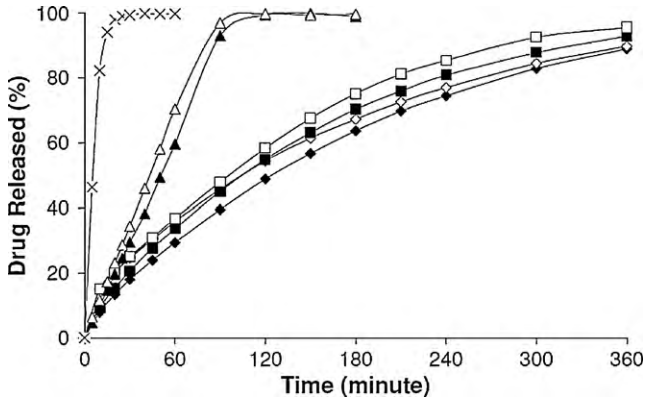

Fig. 10. Dissolution profiles of (×) APAP powder in capsule, (▲) 10APAP-day 1, (△) 10APAP-day 169, (♦) 10APAP10CL15A-hour 1, (◊) 10APAP10CL15A-day 251, (■) 10APAP10CL30B-hour 1, (□) 10APAP10CL30B-day 251.

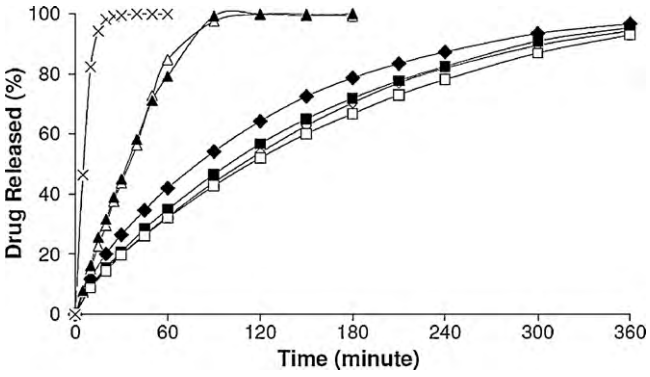

Fig. 11. Dissolution profiles of (×) APAP powder in capsule, (▲) 20APAP-hour 1, (△) 20APAP-day 160, (♦) 20APAP10CL15A-hour 1, (◊) 20APAP10CL15A-day 212, (■) 20APAP10CL30B-hour 1, (□) 20APAP10CL30B-day 212.

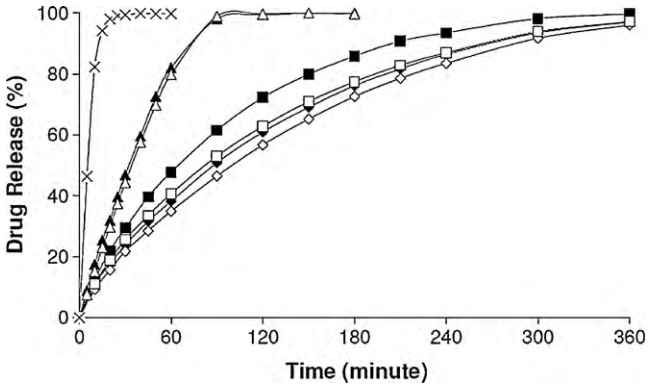

Fig. 12. Dissolution profiles of (×) APAP powder in capsule, (▲) 30APAP-hour 1, (△) 30APAP-day 148, (♦) 30APAP10CL15A-hour 1, (◊) 30APAP10CL15A-day 213, (■) 30APAP10CL30B-hour 1, (□) 30APAP10CL30B-day 213.

Storage time shows little impact on the dissolution rate (Figs. 10–12). For example, the figure shows that the drug release profile on day 1 is essentially the same as that on day 169 for sample 10APAP. A couple of facts should be mentioned in discussing this observation: firstly, in all cases, APAP particles never grow into more than several micrometers. In other words, the morphology does not change with the storage time. Secondly, PEO does not dissolve quickly but swells into a gel in the aqueous medium. Subsequently, the gel gradually dissolves and by the time it disappears, the drug is fully released. The slow dissolution rate of PEO may overshadow any changes in APAP's dissolution rate during storage.

4. Conclusion

APAP–PEO and APAP–PEO–nanoclay with different drug loadings were prepared by a melt mixing process. All samples show extensive APAP recrystallization, independent of the drug loading investigated. For 20 and 30% drug loadings, APAP recrystallizes almost instantaneously upon cooling to room temperature and the recrystallization process slows down to an unappreciable rate after one day. For the 10% drug loading, the recrystallization is slower. However, the size and shape of the APAP particles formed by recrystallization are independent of the drug loading.

The APAP's recrystallization and the dissolution rates are sensitive to the presence of the nanoclays. Nanoclays facilitates APAP's recrystallization and clay-containing samples present much slower dissolution rates compared to both the drug powder and melt-mixed drug–polymer systems. Data analysis of the dissolution results suggests that the drug's release mechanism changes from erosion dominant to diffusion dominant due to the addition of nanoclays. This study suggests that nanoclays may be utilized to tailor

the drug's releasing rate and to improve the drug's stability by dramatically shortening the lengthy recrystallization process.

Acknowledgements

Four of the authors received support from the ongoing US Department of the Army, DAAE30-03-D1015 Advanced Cluster Energetics (ACE^{TM}) Program at New Jersey Institute of Technology (NJIT). This research was financially supported by National Science Foundation under Grant CMMI-0927142.

References

Andrews, G.P., Jones, D.S., Diak, O.A., Mccoy, C.P., Watts, A.B., Mcginity, J.W., 2008. The manufacture and characterisation of hot-melt extruded enteric tablets. Eur. J. Pharm. Biopharm. 69, 264–273.

Breitkreutz, J., 1998. Prediction of intestinal drug absorption properties by three-dimensional solubility parameters. Pharm. Res. 15, 1370–1375.

Campbell, K., Craig, D.Q.M., Mcnally, T., 2008. Poly(ethylene glycol) layered silicate nanocomposites for retarded drug release prepared by hot-melt extrusion. Int. J. Pharm. 363, 126–131.

Coppens, K.A., Hall, M.J., Mitchell, S.A., Read, M.D., 2006. Hypromellose, ethylcellulose, and polyethylene oxide use in hot melt extrusion (cover story). Pharm. Technol. 30, 62–70.

Crank, J., 1975. The Mathematics of Diffusion, 2nd ed. Clarendon Press, Oxford.

De Brabander, C., Vervaet, C., Remon, J.P., 2003. Development and evaluation of sustained release mini-matrices prepared via hot melt extrusion. J. Control. Release 89, 235–247.

De Wet, F.N., Gerber, J.J., Lotter, A.P., Van Der Watt, J.G., Dekker, T.G., 1998. A study of the changes during heating of paracetamol. Drug Dev. Ind. Pharm. 24, 447–453.

Fornes, T.D., Paul, D.R., 2003. Crystallization behavior of nylon 6 nanocomposites. Polymer 44, 3945–3961.

Ghebremeskel, A., Vemavarapu, C., Lodaya, M., 2006. Use of surfactants as plasticizers in preparing solid dispersions of poorly soluble API: stability testing of selected solid dispersions. Pharm. Res. 23, 1928–1936.

Ghebremeskel, A.N., Vemavarapu, C., Lodaya, M., 2007. Use of surfactants as plasticizers in preparing solid dispersions of poorly soluble API: selection of polymer-surfactant combinations using solubility parameters and testing the processability. Int. J. Pharm. 328, 119–129.

Granberg, R.A., Rasmuson, A.C., 1999. Solubility of paracetamol in pure solvents. J. Chem. Eng. Data 44, 1391–1395.

Greenhalgh, D.J., Williams, A.C., Timmins, P., York, P., 1999. Solubility parameters as predictors of miscibility in solid dispersions. J. Pharm. Sci. 88, 1182–1190.

Homminga, D., Goderis, B., Dolbnya, I., Reynaers, H., Groeninckx, G., 2005. Crystallization behavior of polymer/montmorillonite nanocomposites. Part I. Intercalated poly(ethylene oxide)/montmorillonite nanocomposites. Polymer 46, 11359–11365.

Hopfenberg, H.B., Hsu, K.C., 1978. Swelling-controlled, constant rate delivery systems. Polym. Eng. Sci. 18, 1186–1191.

Hülsmann, S., Backensfeld, T., Keitel, S., Bodmeier, R., 2000. Melt extrusion—an alternative method for enhancing the dissolution rate of 17β-estradiol hemihydrate. Eur. J. Pharm. Biopharm. 49, 237–242.

Lang, M., Grzesiak, A.L., Matzger, A.J., 2002. The use of polymer heteronuclei for crystalline polymorph selection. J. Am. Chem. Soc. 124, 14834–14835.

Langer, R., Peppas, N.A., 1983. Chemical and physical structure of polymers as carriers for controlled release of bioactive agents: a review. Rev. Macromol. Chem. Phys. 23, 61–126.

Li, L., Abubaker, O., Shao, Z., 2006. Characterization of poly(ethylene oxide) as a drug carrier in hot-melt extrusion. Drug Dev. Ind. Pharm. 32, 991–1002.

Liu, H., Wang, P., Zhang, X., Shen, F., Gogos, C.G., 2010. Effects of extrusion process parameters on the dissolution behavior of indomethacin in Eudragit® E PO solid dispersions. Int. J. Pharm. 383, 161–169.

Liu, X., Wu, Q., 2002. Non-isothermal crystallization behaviors of polyamide 6/clay nanocomposites. Eur. Polym. J. 38, 1383–1389.

Lloyd, G.R., Craig, D.Q.M., Smith, A., 1997. An investigation into the production of paracetamol solid dispersions in PEG 4000 using hot stage differential interference contrast microscopy. Int. J. Pharm. 158, 39–46.

Loyens, W., Jannasch, P., Maurer, F.H.J., 2005. Effect of clay modifier and matrix molar mass on the structure and properties of poly(ethylene oxide)/cloisite nanocomposites via melt-compounding. Polymer 46, 903–914.

Maiti, P., Nam, P.H., Okamoto, M., Hasegawa, N., Usuki, A., 2002. Influence of crystallization on intercalation, morphology, and mechanical properties of polypropylene/clay nanocomposites. Macromolecules 35, 2042–2049.

Mididoddi, P.K., Repka, M.A., 2007. Characterization of hot-melt extruded drug delivery systems for onychomycosis. Eur. J. Pharm. Biopharm. 66, 95–105.

Özgüney, I., Shuwisitkul, D., Bodmeier, R., 2009. Development and characterization of extended release Kollidon® SR mini-matrices prepared by hot-melt extrusion. Eur. J. Pharm. Biopharm. 73, 140–145.

Peppas, N.A., Korsmeyer, R.W., 1986. Dynamically swelling hydrogels in controlled release applications. In: Peppas, N.A. (Ed.), Hydrogels Med. Pharm., vol. 3. CRC Press, Boca Raton, pp. 109–136.

Peppas, N.A., Sahlin, J.J., 1989. A simple equation for the description of solute release. III. Coupling of diffusion and relaxation. Int. J. Pharm. 57, 169–172.

Prodduturi, S., Manek, R.V., Kolling, W.M., Stodghill, S.P., Repka, M.A., 2005. Solid-state stability and characterization of hot-melt extruded poly(ethylene oxide) films. J. Pharm. Sci. 94, 2232–2245.

Repka, M.A., Prodduturi, S., Stodghill, S.P., 2003. Production and characterization of hot-melt extruded films containing clotrimazole. Drug Dev. Ind. Pharm. 29, 757–765.

Ritger, P., Peppas, N., 1987. A simple equation for description of solute release II. Fickian and anomalous release from swellable devices. J. Control. Release 5, 37–42.

Schilling, S.U., Shah, N.H., Waseem Malick, A., Mcginity, J.W., 2010. Properties of melt extruded enteric matrix pellets. Eur. J. Pharm. Biopharm. 74, 352–361.

Siepmann, J., Peppas, N.A., 2001. Modeling of drug release from delivery systems based on hydroxypropyl methylcellulose (HPMC). Adv. Drug Deliv. Rev. 48, 139–157.

Verhoeven, E., De Beer, T.R.M., Schacht, E., Van Den Mooter, G., Remon, J.P., Vervaet, C., 2009. Influence of polyethylene glycol/polyethylene oxide on the release characteristics of sustained-release ethylcellulose mini-matrices produced by hot-melt extrusion: in vitro and in vivo evaluations. Eur. J. Pharm. Biopharm. 72, 463–470.

Yang, R., Wang, Y., Zheng, X., Meng, J., Tang, X., Zhang, X., 2008. Preparation and evaluation of ketoprofen hot-melt extruded enteric and sustained-release tablets. Drug Dev. Ind. Pharm. 34, 83–89.

Zhang, F., Mcginity, J., 1999. Properties of sustained-release tablets prepared by hot-melt extrusion. Pharm. Dev. Tech. 4, 241–250.